

Transparently manipulating spin-orbit qubit via exact degenerate ground states

Kuo Hai(海阔), Wenhua Zhu(朱文华), Qiong Chen(陈琼), Wenhua Hai(海文华)
Citation: Chin. Phys. B . 2020, 29(8): 083203 . **doi:** 10.1088/1674-1056/ab99b1
Journal homepage: http://cpb.iphy.ac.cn; http://iopscience.iop.org/cpb

What follows is a list of articles you may be interested in

Phase jump in resonance harmonic emission driven by strong laser fields

Yuan-Yuan Zhao(赵媛媛), Di Zhao(赵迪), Chen-Wei Jiang(蒋臣威), Ai-Ping Fang(方爱平), Shao-Yan Gao(高韶燕), Fu-Li Li(李福利)
Chin. Phys. B . 2020, 29(2): 023201 . **doi:** 10.1088/1674-1056/ab5fbf

Up-conversion luminescence tuning in Er^{3+}-doped ceramic glass by femtosecond laser pulse at different laser powers

Wen-Jing Cheng(程文静), Guo Liang(梁果), Ping Wu(吴萍), Shi-Hua Zhao(赵世华), Tian-Qing Jia(贾天卿), Zhen-Rong Sun(孙真荣), Shi-An Zhang(张诗按)
Chin. Phys. B . 2018, 27(12): 123201 . **doi:** 10.1088/1674-1056/27/12/123201

Modulation of multiphoton resonant high-order harmonic spectra driven by two frequency-comb fields

Yuanyuan Zhao(赵媛媛), Di Zhao(赵迪), Chen-Wei Jiang(蒋臣威), Fu-li Li(李福利)
Chin. Phys. B . 2018, 27(5): 053202 . **doi:** 10.1088/1674-1056/27/5/053202

Simulating resonance-mediated two-photon absorption enhancement in rare-earth ions by a rectangle phase modulation

Da-Long Qi(齐大龙), Ye Zheng(郑烨), Wen-Jing Cheng(程文静), Yun-Hua Yao(姚云华), Lian-Zhong Deng(邓联忠), Dong-Hai Feng(冯东海), Tian-Qing Jia(贾天卿), Zhen-Rong Sun(孙真荣), Shi-An Zhang(张诗按)
Chin. Phys. B . 2018, 27(1): 013202 . **doi:** 10.1088/1674-1056/27/1/013202

Polarization control of multi-photon absorption under intermediate femtosecond laser field

Wenjing Cheng(程文静), Pei Liu(刘沛), Guo Liang(梁果), Ping Wu(吴萍), Tianqing Jia(贾天卿), Zhenrong Sun(孙真荣), Shian Zhang(张诗按)
Chin. Phys. B . 2017, 26(8): 083201 . **doi:** 10.1088/1674-1056/26/8/083201

Transparently manipulating spin–orbit qubit via exact degenerate ground states*

Kuo Hai(海阔)†, Wenhua Zhu(朱文华), Qiong Chen(陈琼), and Wenhua Hai(海文华)‡

Department of Physics and Key Laboratory of Low-dimensional Quantum Structures and Quantum Control of Ministry of Education, and Synergetic Innovation Center for Quantum Effects and Applications, Hunan Normal University, Changsha 410081, *China*

(Received 30 March 2020; revised manuscript received 14 May 2020; accepted manuscript online 5 June 2020)

By investigating a harmonically confined and periodically driven particle system with spin–orbit coupling (SOC) and a specific controlled parameter, we demonstrate an exactly solvable two-level model with a complete set of spin-motion entangled Schrödinger kitten (or cat) states. In the undriven case, application of a modulation resonance results in the exact stationary states. We show a decoherence-averse effect of SOC and implement a transparent coherent control by exchanging positions of the probability-density wavepackets to create transitions between the different degenerate ground states. The expected energy consisting of quantum and continuous parts is derived, and the energy deviations caused by the exchange operations are much less than the quantum gap. The results could be directly extended to a weakly coupled single-particle chain for transparently encoding spin–orbit qubits via the robust spin-motion entangled degenerate ground states.

Keywords: transparent coherent control, spin–orbit qubit, exact degenerate ground state, spin–orbit coupling, spin-motion entanglement

PACS: 32.80.Qk, 71.70.Ej, 32.90.+a, 03.65.Ge **DOI:** 10.1088/1674-1056/ab99b1

1. Introduction

The spin–orbit coupling (SOC) can hybridize spin-up and spin-down states to form a spin–orbit qubit.[1–5] The orbital part of the spin-motion entangled states[6–8] can be used for qubit manipulation. Coherent manipulation of electron spin is of critical importance for quantum computing and information processing with spins.[9] The previous investigation has paved the way for manipulating electron spins in an array of quantum dots individually.[10–12] Recently, realization of the laser-induced SOC[13,14] in the low-dimensional cold atom systems opens a broad avenue for studying the many-body quantum dynamics.[15–31] The atomic SOC with equal Rashba and Dresselhaus strengths[13,18] is equivalent to that of an electronic system with equal contribution from Rashba and Dresselhaus SOC.[21] A method of implementing arbitrary forms of SOC in a neutral particle system has also been reported.[32] Particularly, the Rashba and Dresselhaus terms can be transformed into each other under a spin rotation[33,34] and also can be tunable by using a periodic field.[34–36]

A spin–orbit coupled neutral[13,37] or charged[5,38] two-level particle in an external field can be governed by an effective two-level model. The single-particle model also can be derived from a many-particle two-level system,[39–42] by using the Feshbach-resonance technique to make zero interparticle interaction. Analytically solvable driven two-level quantum systems without SOC have continuously attracted considerable attention in diverse areas of physics,[43–52] since exact analytical solutions are invaluable in the contexts of qubit control[49] and can render the control strategies more transparent.[53] The presence of SOC increases the difficult for searching the solvability of the systems and leads the corresponding exact solutions to remain extremely rare.[54,55] Mathematically, a partially differential system allows a general solution with arbitrary functions and a complete solution with arbitrary constants. These arbitrary functions and constants are adjusted and determined by the initial and boundary conditions. The general solution can describe all properties of the system and the complete solution can also describe more physics than any particular solution can. In the previous work, we derived a set of generalized coherent states for a harmonically trapped particle system without SOC,[56–58] which just is a set of complete solutions describing a complete set of Schrödinger kitten (or cat) states. As pointed out in Ref. [59], "a Schrödinger kitten (cat) state is usually defined as a quantum superposition of coherent states with small (big) amplitudes, providing an essential tool for quantum information processing." For an ion system, the similar spin-motion entangled states have been experimentally prepared as the Schrödinger's cat state with two macroscopically separated wavepackets of probability densities.[7,60]

In this paper, we consider a spin–orbit coupled and periodically driven neutral (or charged) particle confined in a

*Project supported by the National Natural Science Foundation of China (Grant Nos. 11204077 and 11475060), the Natural Science Foundation of Hunan Province, China (Grant No. 2019JJ10002), the Hunan Provincial Hundred People Plan, China (2019), and the Science and Technology Plan Project of Hunan Province, China.

†Corresponding author. E-mail: ron.khai@gmail.com

‡Corresponding author. E-mail: whhai2005@aliyun.com

© 2020 Chinese Physical Society and IOP Publishing Ltd

harmonic trap. We define and manage the controlled Raman–Zeeman angle (or the orientation of the static magnetic field) θ to match the SOC-dependent phase $\phi = \arctan\frac{\alpha_{\rm R}}{\alpha_{\rm D}}$ with $\alpha_{\rm R(D)}$ being the Rashba (Dresselhaus) SOC strength,[5] which is called formally the SOC phase-locked condition. Under this condition, we establish an exactly solvable two-level model and construct a complete set of exact Schrödinger kitten states with spin-motion entanglement, which contain some degenerate ground states with norms of motional states being a kind of oscillating wavepackets. Further application of a modulation resonance with the defined Raman–Zeeman (or magnetic field) strength being modulated to fit the trap frequency leads to the undriven stationary double packets. The decoherence-averse effect of SOC and the coherent control of quantum operations based on interchanges of the wavepackets are revealed transparently, which shift the system between different degenerate ground states. The expected energy consists of a quantum part and a continuous one, and the energy deviations caused by the exchange operations are much less than the quantum gap such that the coherent operation is robust against perturbations and interactions with the environment. The exact results could be treated as the leading-order ones to directly extend to a weakly coupled nanowire quantum-dot-electron chain (or an array of neutral particles separated from each other by different optical wells[61,62] with weak neighboring coupling) for encoding the spin–orbit qubits.

2. A complete set of spin-motion entangled Schrödinger kitten states

We consider a one-dimensional (1D) harmonically confined and periodically driven[21,40] two-level particle with Rashba–Dresselhaus coexisting SOC,[5,32,38,42] which is governed by the effective Hamiltonian[5]

$$\begin{aligned} H &= H_0 + \alpha_{\rm D}\sigma_x p_x + \alpha_{\rm R}\sigma_y p_x + \frac{1}{2}g_0(\sigma_x\cos\theta + \sigma_y\sin\theta), \\ H_0 &= -\frac{1}{2}\frac{\partial^2}{\partial x^2} + \frac{1}{2}x^2 + \varepsilon x\cos(\Omega t). \end{aligned} \tag{1}$$

Here we have adopted the natural unit system with $\hbar = m = \omega = 1$, so that time, space, and energy are normalized in units of ω^{-1}, $L_h = \sqrt{\hbar/(m\omega)}$, and $\hbar\omega$ with m and ω being the particle mass and trapped frequency. The $p_x = -{\rm i}\partial/\partial x$ denotes the momentum operator, $\alpha_{\rm R(D)}$ is the Rashba (Dresselhaus) SOC strength,[5,32,38,42] and $\sigma_{x(y)}$ is the $x(y)$ component of the Pauli matrix. For a charged particle,[5] g_0 is equal to $g_{\rm e}\mu_{\rm B}B$ with $g_{\rm e}$ being the gyromagnetic ratio,[33] $\mu_{\rm B}$ is the Bohr magneton, B and θ represent the strength and orientation of the static magnetic field. For a neutral atom,[13,37] $g_0\cos\theta$ and $g_0\sin\theta$ are, respectively, the Raman coupling strength and the tunable detuning behaving as a Zeeman field.[21,32] Here, for convenience, we have expressed the Raman and Zeeman parameters in terms of two new ones g_0 and θ without loss of generality, which are defined as the Raman–Zeeman strength and angle, respectively. Clearly, the zero Raman–Zeeman (or magnetic field) angle means the zero detuning and the Raman coupling strength equating g_0 (or magnetic field being in x direction with strength g_0). The spin-dependent terms can be adjusted by a spin rotation.[33,34] The driving parameters ε and Ω are the amplitude and frequency of the ac field, and the related linear potential can be produced by a periodic magnetic field gradient for the neutral atom[63,64] or simply is an ac electric potential for a charged particle.

Applying the usual state vector $|\psi(t)\rangle = \frac{1}{\sqrt{2}}[|\psi_+(t)\rangle|\uparrow\rangle + |\psi_-(t)\rangle|\downarrow\rangle]$, the space-dependent state vector reads[7,26,27]

$$|\psi(x,t)\rangle = \langle x|\psi(t)\rangle = \frac{1}{\sqrt{2}}\Big[\psi_+(x,t)|\uparrow\rangle + \psi_-(x,t)|\downarrow\rangle\Big] \tag{2}$$

with $\psi_\pm(x,t) = \langle x|\psi_\pm(t)\rangle$ being the normalized motional states entangling the corresponding spin states $|\uparrow\rangle = \begin{pmatrix}1\\0\end{pmatrix}$ and $|\downarrow\rangle = \begin{pmatrix}0\\1\end{pmatrix}$, respectively. Although $|\psi_\pm(t)\rangle$ may be expanded in terms of a set of orthonormal basic kets with time-dependent expansion coefficients,[6] here we will seek the exact complete solutions $\psi_\pm(x,t)$. Therefore, the spin-motion entanglement of Eq. (2) requires the linear independencies[26,27,58] of $\psi_+(x,t)$ and $\psi_-(x,t)$. The probabilities of the particle being in spin states $|\uparrow\rangle$ and $|\downarrow\rangle$ read $P_\pm(t) = \frac{1}{2}\int|\psi_\pm(x,t)|^2{\rm d}x$. The maximal spin-motion entanglement can be associated with[58] $P_+ = P_- = 1/2$. Applying Eqs. (1) and (2) to the Schrödinger equation ${\rm i}\partial|\psi(x,t)\rangle/\partial t = H|\psi(x,t)\rangle$ yields the matrix equation

$$\begin{aligned} {\rm i}\frac{\partial}{\partial t}\begin{pmatrix}\psi_+\\ \psi_-\end{pmatrix} &= H_0\begin{pmatrix}\psi_+\\ \psi_-\end{pmatrix} - {\rm i}\alpha\frac{\partial}{\partial x}\begin{pmatrix}{\rm e}^{-{\rm i}\phi}\psi_-\\ {\rm e}^{{\rm i}\phi}\psi_+\end{pmatrix} \\ &\quad + \frac{g_0}{2}\begin{pmatrix}{\rm e}^{-{\rm i}\theta}\psi_-\\ {\rm e}^{{\rm i}\theta}\psi_+\end{pmatrix}, \\ \alpha &= \sqrt{\alpha_{\rm D}^2 + \alpha_{\rm R}^2}, \quad \phi = \arctan\frac{\alpha_{\rm R}}{\alpha_{\rm D}}, \end{aligned} \tag{3}$$

where we have taken the definitions of the SOC strength and SOC-dependent phase as[5] α and ϕ for the Rashba–Dresselhaus SOC coexistence system. In order to apply the SOC phase-locked condition for deriving the exact solutions of the matrix equation, we make the function transformations

$$\begin{aligned} &\psi_\pm(x,t) = \psi_{\pm,l}(x,t) \\ &= {\rm e}^{\mp{\rm i}\phi/2}[u(x,t){\rm e}^{-{\rm i}(\alpha x + l\pi/2)} \pm v(x,t){\rm e}^{{\rm i}(\alpha x + l\pi/2)}] \end{aligned} \tag{4}$$

for $l = 0,1,2,\ldots$. Inserting Eq. (4) into Eq. (3), then multiplying the first line of the matrix equation by ${\rm e}^{{\rm i}(\phi/2+\alpha x+l\pi/2)}$ and multiplying the second line of the equation by ${\rm e}^{-{\rm i}(\phi/2+\alpha x+l\pi/2)}$, we obtain

$$\mathrm{i}\frac{\partial}{\partial t}\begin{pmatrix}u\\v\end{pmatrix}=\left(H_0-\frac{\alpha^2}{2}\right)\begin{pmatrix}u\\v\end{pmatrix}+\frac{1}{2}g_0\begin{pmatrix}\mathrm{e}^{-\mathrm{i}(\theta-\phi)}[u-v\mathrm{e}^{\mathrm{i}(2\alpha x+l\pi)}]+\mathrm{e}^{\mathrm{i}(\theta-\phi)}[u+v\mathrm{e}^{\mathrm{i}(2\alpha x+l\pi)}]\\ \mathrm{e}^{-\mathrm{i}(\theta-\phi)}[u\mathrm{e}^{-\mathrm{i}(2\alpha x+l\pi)}-v]-\mathrm{e}^{\mathrm{i}(\theta-\phi)}[u\mathrm{e}^{-\mathrm{i}(2\alpha x+l\pi)}+v]\end{pmatrix}. \tag{5}$$

For an arbitrary angle θ, the final term of Eq. (5) cannot be decoupled, so it is hard to construct an exact solution of the system. The corresponding perturbed solution has been considered in Ref. [5] that leads to some interesting results. Here we are interested in the formal SOC phase-locked case $\theta=\phi=\arctan\frac{\alpha_{\mathrm{R}}}{\alpha_{\mathrm{D}}}\to\phi_0+j\pi$ for $j=0,1,2,\ldots$ and $\phi_0\in[0,\frac{\pi}{2}]$, which can be realized experimentally for the fixed SOC strengths α_{R} and α_{D} by selecting the proper Raman–Zeeman angle (or orientation of magnetic field). In such a selection, the orientation angle θ can take different values associated with the different number j, because of the multivaluedness of the inverse tangent function. Under the SOC phase-locked condition, equation (5) becomes the decoupled equation

$$\mathrm{i}\frac{\partial}{\partial t}\begin{pmatrix}u\\v\end{pmatrix}=\left[H_0(x,t)-\frac{\alpha^2}{2}+g_0\sigma_z\right]\begin{pmatrix}u\\v\end{pmatrix}\quad\text{for}\quad\theta=\phi, \tag{6}$$

where σ_z is z component of the Pauli matrix. Equation (6) is just the exactly solvable two-level model of the effective Hamiltonian $H_{\mathrm{eff}}=H_0-\alpha^2/2+g_0\sigma_z$. Given Eq. (6), we find that the integer l in state (4) becomes independent of the symmetry characterised by the potential in H_0, due to the independence of functions u,v on l. It is the SOC phase-lock that makes such an independence, so the degeneracy of Eq. (4) associated with l could be SOC-dependent.

After making the new function transformations

$$u=\frac{c_u}{\sqrt{2}}f_u(x,t)\,\mathrm{e}^{\mathrm{i}(\alpha^2/2-g_0)t},\quad v=\frac{c_v}{\sqrt{2}}f_v(x,t)\,\mathrm{e}^{\mathrm{i}(\alpha^2/2+g_0)t} \tag{7}$$

with c_u and c_v being the complex constants determined by the normalization and initial conditions, the decoupled Eq. (6) gives the time-dependent Schrödinger equation

$$\mathrm{i}\frac{\partial f_{u(v)}}{\partial t}=H_0 f_{u(v)}$$

of a driven harmonic oscillator with the exact complete solutions being the orthonormal generalized coherent states[56–58]

$$\begin{aligned}
f_{u(v)}&=f_{n_{u(v)}}=R_{n_{u(v)}}(x,t)\,\mathrm{e}^{\mathrm{i}\Theta_{n_{u(v)}}(x,t)},\\
\Theta_{n_{u(v)}}&=-\left(\frac{1}{2}+n_{u(v)}\right)\chi(t)+b_{u(v)2}x+\frac{\dot\rho}{2\rho}x^2+\gamma_{u(v)}(t),\\
R_{n_{u(v)}}&=\left(\frac{\sqrt{c_0}}{\sqrt{\pi}2^{n_{u(v)}}n_{u(v)}!\rho}\right)^{\frac{1}{2}}H_{n_{u(v)}}[\xi_{u(v)}]\,\mathrm{e}^{-\frac{1}{2}\xi^2_{u(v)}},\\
\xi_{u(v)}&=\frac{\sqrt{c_0}}{\rho(t)}x-\frac{b_{u(v)1}(t)\rho(t)}{\sqrt{c_0}},
\end{aligned} \tag{8}$$

for $n_u,n_v=0,1,2,\ldots$ with $R_{n_{u(v)}}(x,t)$ and $\Theta_{n_{u(v)}}(x,t)$ being the real functions and $H_{n_{u(v)}}[\xi_{u(v)}]$ the Hermite polynomial of the space–time combined variable $\xi_{u(v)}(x,t)$. In Eq. (8), the real functions $\rho(t),\chi(t)$, $\gamma_{u(v)}(t),b_{u(v)1}(t)$, and $b_{u(v)2}(t)$ have the forms[56–58]

$$\begin{aligned}
\varphi_{1,2}(t)&=A_{1,2}\cos(t+B_{1,2}),\quad\rho(t)=\sqrt{\varphi_1^2+\varphi_2^2},\\
\chi(t)&=\arctan\left(\frac{\varphi_2}{\varphi_1}\right),\\
b_{u(v)1}(t)&=\frac{\varepsilon}{\rho^2(t)}\Big[\varphi_1(t)\int_0^t\varphi_2(\tau)\cos(\Omega\tau)\,\mathrm{d}\tau\\
&\quad-\varphi_2(t)\int_0^t\varphi_1(\tau)\cos(\Omega\tau)\,\mathrm{d}\tau\Big]\\
&\quad+b_{u(v)1}(0)\varphi_1(t)+b_{u(v)2}(0)\varphi_2(t),\\
b_{u(v)2}(t)&=\frac{\varepsilon}{\rho^2(t)}\Big[-\varphi_1(t)\int_0^t\varphi_1(\tau)\cos(\Omega\tau)\,\mathrm{d}\tau\\
&\quad-\varphi_2(t)\int_0^t\varphi_2(\tau)\cos(\Omega\tau)\,\mathrm{d}\tau\Big]\\
&\quad+b_{u(v)2}(0)\varphi_1(t)-b_{u(v)1}(0)\varphi_2(t),\\
\gamma_{u(v)}(t)&=\frac{1}{2}\int_0^t[b^2_{u(v)1}(\tau)-b^2_{u(v)2}(\tau)]\,\mathrm{d}\tau+\gamma_{u(v)}(0).
\end{aligned} \tag{9}$$

Here the initial constant sets $S_{u(v)}=[\gamma_{u(v)}(0),\ b_{u(v)1}(0),\ b_{u(v)2}(0),A_{1,2},B_{1,2}]$ are determined by the forms of the initial states[58] which could be prepared experimentally.[7,60] Then the solutions $f_{u(v)}=f_{n_{u(v)}}[S_{u(v)},x,t]$ are determined by the sets $S_{u(v)}$ for fixed quantum numbers $n_{u(v)}$.

Applications of Eq. (7) to Eq. (4) result in new forms of the exact complete solutions of Eq. (3) as

$$\begin{aligned}
\psi_{\pm,ln_un_v}(x,t)&=\frac{1}{\sqrt{2}}\mathrm{e}^{\frac{\mathrm{i}}{2}(\alpha^2t\mp\phi-l\pi)}[c_uf_{n_u}\,\mathrm{e}^{-\mathrm{i}(\alpha x+g_0t)}\\
&\quad\pm c_vf_{n_v}\,\mathrm{e}^{\mathrm{i}(\alpha x+g_0t+l\pi)}].
\end{aligned} \tag{10}$$

In Eq. (10), the quantum numbers $n_{u(v)}$ and integer l are independent of the parameters in system (1). The solutions $f_{n_{u(v)}}(x,t)$ of Eq. (8) can be the eigenstates of a harmonic oscillator for the undriven case with $\varepsilon=0$ and the generalized coherent states for any driving strength,[56–58] which lead to different forms of Eq. (10) and the corresponding rich physics. Obviously, for any nonzero function pair $f_{u(v)}$ and nonzero constants c_u,c_v,α,g_0, the solutions $\psi_{+,ln_un_v}(x,t)$ and $\psi_{-,ln_un_v}(x,t)$ are linearly independent, so the superposition state (2) is spin-motion entangled. It is important to note that in Eqs. (8) and (10), $f_{n_{u(v)}}$ depends only on the ac driving and trapping field, and is independent of the SOC, the Raman–Zeeman parameters (or static magnetic field), and the integer l. Therefore, we can conveniently manipulate the motional states (10) by independently adjusting the driving and the initial constants to select the exact solutions of Eq. (8), and by independently tuning the SOC parameters α and Raman–Zeeman (or magnetic field) parameter g_0 for a fixed $\phi=\theta$. Applying Eq. (10) to Eq. (2) and noticing $\psi_{\pm,ln_un_v}(x,t)=\langle x|\psi_{\pm,ln_un_v}\rangle$, we arrive at the orthonormal complete set of the exact superposition states, $|\psi_{ln_un_v}\rangle=\frac{1}{\sqrt{2}}[|\psi_{+,ln_un_v}\rangle|\uparrow\rangle+|\psi_{-,ln_un_v}\rangle|\downarrow\rangle]$.

By making use of the orthonormalization of $f_{n_u(n_v)}$ and Eqs. (8)–(10), the expected energy of the system reads[56,57]

$$E_{n_un_v}(t) = \mathrm{i}\langle\psi_{ln_un_v}|\frac{\partial}{\partial t}|\psi_{ln_un_v}\rangle = \frac{\mathrm{i}}{2}\int_{-\infty}^{\infty}\left(|c_u|^2 f_{n_u}\frac{\partial f_{n_u}}{\partial t}+|c_v|^2 f_{n_v}\frac{\partial f_{n_v}}{\partial t}\right)\mathrm{d}x-\frac{\alpha^2}{2}.$$

Any term of the above integral has been calculated carefully in Refs. [56,57]. Application of the calculated result leads to

$$\begin{aligned}&E_{n_un_v}(t)\\ &=-\frac{\alpha^2}{2}-\frac{1}{2}\int_{-\infty}^{\infty}\left(|c_u|^2\dot{\Theta}_{n_u}R_{n_u}^2+|c_v|^2\dot{\Theta}_{n_v}R_{n_v}^2\right)\mathrm{d}x\\ &=\left(\frac{1}{2}+n_u\right)\frac{|c_u|^2}{2}+\left(\frac{1}{2}+n_v\right)\frac{|c_v|^2}{2}+\frac{\varepsilon}{2}(x_u+x_v)\cos(\Omega t)\\ &\quad+\frac{1}{4}\left[|c_u|^2(x_u^2+p_u^2)+|c_v|^2(x_v^2+p_v^2)\right]-\frac{\alpha^2}{2}.\end{aligned}\tag{11}$$

Here we have used the expressions $x_{u(v)}=\int R_{n_{u(v)}}^2(x,t)x\mathrm{d}x$ and $p_{u(v)}=\dot{x}_{u(v)}$ in which both can be corresponding to the classical coordinates and momenta for the generalized coherent states $f_{n_{u(v)}}(x,t)$ of a harmonic oscillator,[56,57] while they vanish for any time-independent eigenstate of a harmonic oscillator with $\varepsilon=0$ and the normalization constants obeying $|c_u|=|c_v|=1$. The energy is a summation of the quantum part $E_\mathrm{q}=\frac{1}{2}(\frac{1}{2}+n_u)|c_u|^2+\frac{1}{2}(\frac{1}{2}+n_v)|c_v|^2$ and the other part of continuous evolution in time. When the ac driving is switched off, the energy $E_{n_un_v}(t)$ becomes time-independent. The ground state is defined as the state with the lowest E_q for the nonzero constants $c_{u(v)}$. Thus the energy of ground states is the instantaneous lowest one for a set of given parameters and initial conditions. It can be time-dependent or time-independent, depending on whether the driving vanishing. It is interesting to see that the states of Eq. (10) depend on the integer l but the energy of Eq. (11) is independent of l. Therefore, for a set of fixed quantum numbers n_u,n_v, different integer l labels different degenerate states of Eq. (2). Differing from the usual relation between the degeneracy and symmetry in quantum mechanics, the degeneracy described by the integer l is independent of the symmetry of H_0 such that it is a symmetry-independent quantum degeneracy. In the 2D case of Ref. [65], the symmetry-independent degeneracy may mean the topological degeneracy.

Given Eqs. (10) and (8), the wavepackets of probability densities are described by the squared norms

$$\begin{aligned}&|\psi_{\pm,ln_un_v}(x,t)|^2=\frac{1}{2}\left(|c_u|^2R_{n_u}^2+|c_v|^2R_{n_v}^2\right)\pm D_{uv},\\ &D_{uv}(x,t)=|c_uc_v|R_{n_u}R_{n_v}\\ &\qquad\times\cos[\Theta_{n_u}-\Theta_{n_v}-2(\alpha x+g_0t)-l\pi-\phi']\end{aligned}\tag{12}$$

of the motional state functions, where constant ϕ' is the phase difference, $\phi'=\arg c_v-\arg c_u$. The term $D_{uv}(x,t)$ describes the phase coherence and signs "±" imply different coherent effects for the different motional states. The phase coherence is protected by the SOC, since for arbitrary $\Theta_{n_u}(x,t)$ and $\Theta_{n_v}(x,t)$, the space dependence of coherence-dependent function $D_{uv}(x,t)$ can be kept at all time only for the nonzero SOC strength α. We can identify the phase coherence as the heart for controlling quantum wavepackets described by Eq. (12). The orthonormalization of Eq. (8) means that the probabilities of the particle being in spin states $|\uparrow\rangle$ and $|\downarrow\rangle$ obey $P_{+,ln_un_v}(t)+P_{-,ln_un_v}(t)=\frac{1}{2}\int(|c_u|^2R_{n_u}^2+|c_v|^2R_{n_v}^2)\mathrm{d}x=\frac{1}{2}(|c_u|^2+|c_v|^2)=1$, which confines the normalization constants c_u,c_v. The maximal spin-motion entanglement[58] with $P_+=P_-=1/2$ implies $|c_u|=|c_v|=1$. Therefore, in such a case, the probabilities of the particle occupying spin states $|\uparrow\rangle$ and $|\downarrow\rangle$ become

$$P_\pm(t)=\frac{1}{2}\int|\psi_\pm(x,t)|^2\mathrm{d}x=\frac{1}{2}\left[1\pm\int D_{uv}(x,t)\mathrm{d}x\right].$$

Given c_u, c_v, n_u, and n_v, for a fixed l, equation (12) contains two different wavepackets distinguished by $\pm D_{uv}(x,t)$, while for a fixed sign of "±", equation (12) also contains only a pair of different wavepackets $|\psi_{\pm,ln_un_v}|^2$ with even l or odd l, respectively. Clearly, equation (12) shows $|\psi_{+,ln_un_v}|^2=|\psi_{-,l'n_un_v}|^2$ with l and l' possessing different odevity. Therefore, equations (10) and (2) mean that $|\psi_{ln_un_v}\rangle$ and $|\psi_{l'n_un_v}\rangle$ are two different degenerate states associated with some interchanges of wavepackets. The wavepackets described by $|\psi_{+,ln_un_v}|^2$ and $|\psi_{-,ln_un_v}|^2$ may be spatially separated and be centred at different positions, $x_{\pm,u(v)}=\int|\psi_{\pm,ln_un_v}|^2x\mathrm{d}x$. This means that equation (2) is a complete set of Schrödinger kitten states[59] which includes the degenerate ground states with the lowest quantum level $E_\mathrm{q}=\frac{1}{2}(1+n_u|c_u|^2+n_v|c_v|^2)$ and different initial constants.

Let us extend the definition of a cat state at a selected time (e.g., the initial time) with the macroscopically separated wavepackets[7] to the definition of a "kitten state" with smaller maximal distance between two wavepackets,[59] where $|\uparrow\rangle$ and $|\downarrow\rangle$ refer to the internal states of an atom that has not and has radioactively decayed, while the right and left wavepackets refer to the live (☺) and dead (☹) states of a kitten. We can formally write a ground state of Eq. (2) as a Schrödinger kitten state of even l as[7] $|\psi_{ln_un_v}\rangle=\frac{1}{\sqrt{2}}(|☺\rangle|\uparrow\rangle+|☹\rangle|\downarrow\rangle)$ with the right and left wavepackets being described by the squared norms $|\langle x|☺\rangle|^2$ and $|\langle x|☹\rangle|^2$ which are associated with the internal states $|\uparrow\rangle$ and $|\downarrow\rangle$, respectively. Then its degenerate ground state of odd l' reads $|\psi_{l'n_un_v}\rangle=\frac{1}{\sqrt{2}}(|☺\rangle|\uparrow\rangle+|☹\rangle|\downarrow\rangle)$ with exchange of wavepacket positions or equivalent spin flip, which is called a "ill kitten" transferring from near-dead to alive when the atom has radioactively decayed. For a group of fixed quantum numbers n_u, n_v and integer l we will demonstrate that the positions of the wavepacket pair $|\psi_{+,ln_un_v}(x,t)|^2$

and $|\psi_{-,ln_un_v}(x,t)|^2$ can be exchanged by applying the ac field. The name "Schrödinger kitten" of the superposition states is determined only by the spatially separated norms of the motional states at a selected time such that it can be related to many kitten states distinguished by the different phases. The degeneracy of the ground kitten states is not based on simple symmetry consideration and the analogues of the 2D case is a topological degeneracy[65] thereby. Particularly, for some values of SOC strength, the motional states of the kittens and ill kittens may exist zero-density nodes. These nodes are associated with the singular points of the phase gradients at which the phases of the states occur jumps.[66]

3. Exchanging density wavepackets of degenerate ground states

Generally, equations (11) and (12) imply that the expected energy and the probability densities are periodic functions of time. However, in Eq. (10), the phases $\arg\psi_{\pm,ln_un_v}$ of $\psi_{\pm,ln_un_v}(x,t)$ are obviously different for signs "+" and "−", and are aperiodic in time. The periodically varying norms and the aperiodically varying phases lead to that transitions between the degenerate ground states can be manipulated by exchanging positions of the density wavepackets. Let us take a simple example with $|c_u| = |c_v| = 1, n_u = n_v = l = 0$ and the initial constant set $S_{u(v)} = [\gamma_{u(v)}(0) = b_{u(v)2}(0) = 0, b_{u1}(0) = -b_{v1}(0) = b_0, A_1 = A_2 = A, B_1 = 0, B_2 = -\pi/2]$ to demonstrate the interchange property of the Schrödinger kittens. These constants make Eqs. (9) and (10) have the explicit form, as in Eqs. (A1) and (A2) of Appendix A, where the periodic norms and aperiodic phases are exhibited. Applying Eqs. (A1) and (A2) to Eq. (12), we display the spatiotemporal evolutions of the density wavepackets in Fig. 1 for the parameters $\alpha = 0.2, \phi' = 3, \varepsilon = 0.2, \Omega = 2, g_0 = 0.1$, and $b_0 = 1$. We can see the complicated spatiotemporal evolutions and the time periodicity as shown in Fig. 1(a) with the expectation values of the wavepackets' coordinates given by Eq. (12) as $x_\pm(t) = \int |\psi_{\pm,ln_un_v}(x,t)|^2 x\mathrm{d}x$. Applying Eqs. (A1) and (A2) yields $x_+(t) = -x_-(t)$, namely, the spin-up wavepacket and spin-down wavepacket move in the opposite directions. In Fig. 1(b) we show the ill kitten state at time $t = 5.0(\omega^{-1})$ and kitten state at time $t = 13.8(\omega^{-1})$ with interchange of the wavepacket positions. In both cases, the two separated peaks have a distance in order of $L_h = \sqrt{\hbar/(m_e\omega)}$. In the time interval $t \in (5.0, 13.8)$, there exist many pairs of wavepackets with different shapes. The same wavepackets will periodically appear and the corresponding states may change their phases aperiodically. Thus the interchanges of wavepackets make the norms and phases of $\psi_{\pm,000}(x,t)$ to change their spatiotemporal distributions asynchronously that results in the change of the spin-motion entangled state.

Note that at any moment t_0, the probabilities $P_\pm(t_0) = \int |\psi_{\pm,000}(x,t_0)|^2 \mathrm{d}x$ of the particle being in different spin states are equal to the areas between the wavepacket curves and the x axis. The spatial distributions in Fig. 1(b) mean that the symmetrical kitten and ill kitten states have the same probability $P_\pm(5.0) = P_\pm(13.8) = 1/2$. Obviously, for some time in interval $(5, 13.8)$, figure 1(a) has asymmetrical probability distributions corresponding to $P_+ \ll P_-$ or $P_- \ll P_+$. The result means more possibilities of the spin manipulation by switching off the ac field at different time.

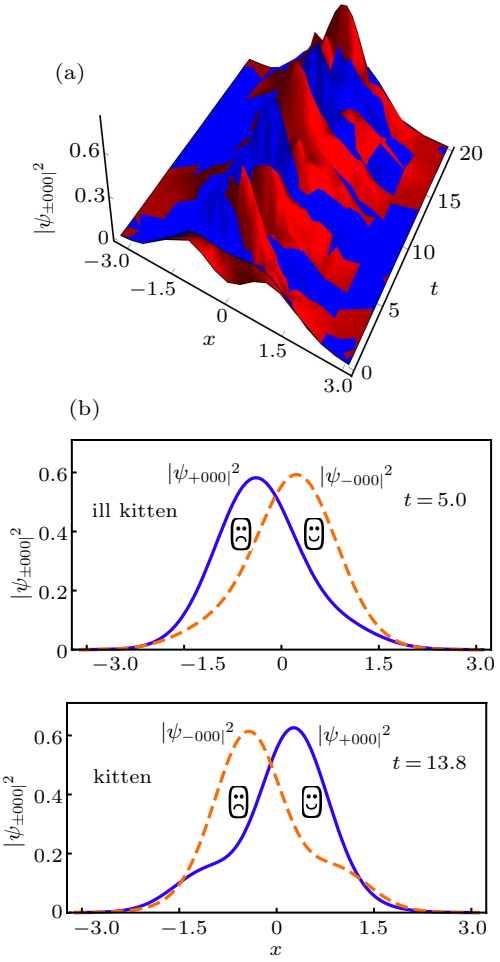


Fig. 1. Spatiotemporal evolutions of the deformed wavepackets described by the probability density $|\psi_{\pm,000}(x,t)|^2$ of Eq. (12) with complicatedly oscillating positions which are described by the time-varying wave-peaks. Hereafter, the blue color and solid curves are associated with sign "+", the red color and dashed curves correspond to sign "−", and the right and left wavepackets $|\langle x|\text{☺}\rangle|^2$ and $|\langle x|\text{☹}\rangle|^2$ in a plot are always labeled by the live ☺ and dead ☹, respectively. When the packet $|\psi_{+,000}(x,t)|^2$ is localized on the right or left side, we call the superposition state the kitten state or ill kitten state. All the quantities plotted in the figures of this paper are dimensionless.

In order to produce regular oscillations of the wavepackets for exchanging their positions at given time, we can apply a $\pi/2$ pulse of Ramsey type experiment to rotate the state vector (2) to the form[67] $|\psi'_{ln_un_v}\rangle = \frac{1}{\sqrt{2}}[|\psi'_{+,ln_un_v}\rangle|\uparrow\rangle + |\psi'_{-,ln_un_v}\rangle|\downarrow\rangle]$ with $|\psi'_{\pm,ln_un_v}\rangle = \frac{1}{\sqrt{2}}(|\psi_{+,ln_un_v}\rangle \pm |\psi_{-,ln_un_v}\rangle$. Thus the probability amplitudes of the particle being in spin states $|\uparrow\rangle$ and $|\downarrow\rangle$ become the new wave functions

$$\psi'_{\pm,ln_un_v}(x,t) = \frac{1}{\sqrt{2}}[\psi_{+,ln_un_v}(x,t) \pm \psi_{-,ln_un_v}(x,t)]. \quad (13)$$

Then applications of Eq. (10) with $c_u = c_v = 1$ to Eq. (13) give explicit forms of the wave functions [see Eq. (B1) in Appendix B]. The corresponding wavepackets are described by the probability densities which obey the normalization requirement $|\psi'_{+,l n_u n_v}|^2 + |\psi'_{-,l n_u n_v}|^2 = R^2_{n_u} + R^2_{n_v}$. A careful calculation can prove that this rotation keeps the expectation value of energy (11) and the independence of energy on the parameters ϕ and l. Therefore, $|\psi'_{l n_u n_v}\rangle$ and $|\psi'_{l' n_u n_v}\rangle$ are also two degenerate states with different $|\psi'_{\pm,l n_u n_v}\rangle$ and $|\psi'_{\pm,l' n_u n_v}\rangle$, while for a fixed l the Raman–Zeeman (or magnetic field) angle transformation from $\theta = \phi$ to $\theta = \phi + \pi$ causes transition between two degenerate states with exchange between $\psi'_{+,l n_u n_v}(x,t)$ and $\psi'_{-,l n_u n_v}(x,t)$ (see Appendix B), meaning the spin flip. We are interested in the exact instantaneous ground state $\psi'_{\pm,000}(x,t)$ with $n_u = n_v = l = 0$. Adopting the parameters $\alpha = 0.1, g_0 = 0.5, b_0 = 1, \varepsilon = 0.2, \Omega = 2$, and $\phi = 0.1$, from the norms of Eq. (13) [with explicit forms of Eq. (B2) in Appendix B] we plot the spatiotemporal evolutions of the wavepackets $|\psi'_{\pm,000}(x,t)|^2$ in Fig. 2(a), where the wavepackets approximately keep shape and perform regularly 1D oscillations with expected coordinates $x'_{\pm}(t) = \int |\psi'_{\pm,000}(x,t)|^2 x \mathrm{d}x$ obeying $x'_{+}(t) = -x'_{-}(t)$. The governing initial state is a kitten state and the ill kitten state appears at $t = 2.6, \ldots$, as shown in Fig. 2(b). In the time internal $t \in [t_\mathrm{i} = 0, t_\mathrm{f} = 2.6]$, the interchange of wavepackets $|\langle x|\text{☺}\rangle|^2$ and $|\langle x|\text{☹}\rangle|^2$ leads to that the two motional states exchange norms with each other and accumulate different phases, as formulated in the time evolution Eqs. (14) and (15). We also find numerically that the increase of the initial constant b_0 can lengthen the maximal distance between wavepackets, while the latter can be selected by preparing the initial wavepackets.[7,60]

The degenerate ground states can be manipulated by a field-driven interchange of wavepackets at an appropriate time interval $t \in [t_\mathrm{i}, t_\mathrm{f}]$, by using the time-evolution operator $U(t_\mathrm{f}, t_\mathrm{i}) = \mathrm{e}^{-\mathrm{i}H(t_\mathrm{f} - t_\mathrm{i})}$ to act on the initial superposition state $|\psi'_{l n_u n_v}(t_\mathrm{i})\rangle$ which approximately fits a stationary ground state $|\psi_{l n_u n_v}\rangle$ of Eq. (2) for a undriven system. We switch on the ac electric field in the original Hamiltonian (1) at t_i and switch it off at t_f, creating a quantum transition between the initial and final degenerate stationary states with the desired occupying probabilities of the different spin states. The phase difference $\arg \psi'_{-,l n_u n_v} - \arg \psi'_{+,l n_u n_v}$ of $\psi'_{\pm,l n_u n_v}(x,t)$ is an aperiodic function of time, and the accumulated phase difference from the initial time t_i to the final time t_f can be nonzero that leads to interchanges of the wavepackets with final state $|\psi'_{l n_u n_v}(t_\mathrm{f})\rangle$ completely differing from the initial states. Such controlled wavepacket interchanges can be performed locally for any particle in an array of quantum-well trapped particles.[9] According to Eq. (B2), we also can adjust the Raman–Zeeman (or magnetic field) angle from $\theta = \phi = 0.1$ to $\theta = \phi = 0.1 + \pi$ to produce the wavepacket exchange between $|\psi'_{+,000}(x,t)|^2$ and $|\psi'_{-,000}(x,t)|^2$, which does not show here. For an array of trapped charged particles, such magnetically controlling wavepacket interchanges can be performed simultaneously in a wide range.[5]

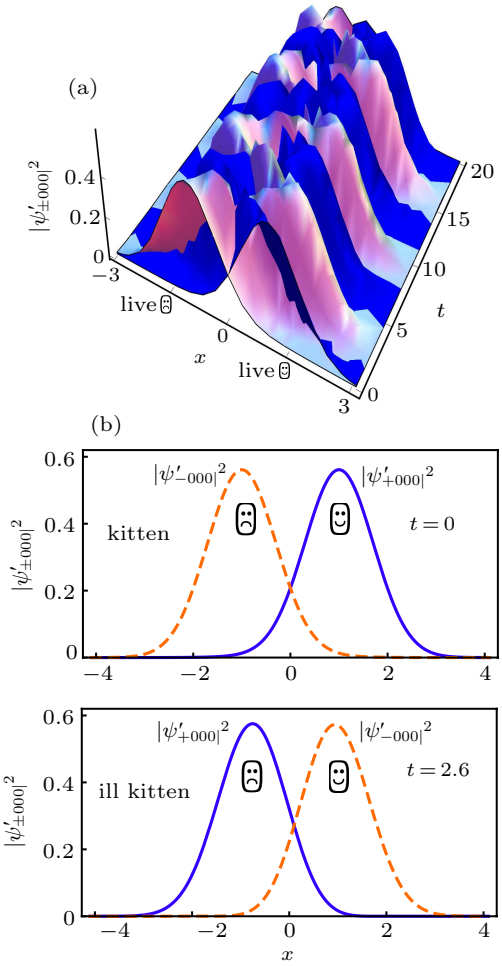


Fig. 2. Spatiotemporal evolutions of the wavepackets $|\psi'_{\pm,000}(x,t)|^2$ from Eq. (13) with regular oscillations. Starting with a kitten state, the wavepacket pair approximately keeps their shapes and periodically oscillates. In an oscillating period, the wavepackets can go through many kitten states similar to the initial state in Fig. 1(b) and ill kitten states similar to the state at $t = 2.6$ in Fig. 2(b) with different distances between the wavepackets, which can be extracted by the ac field manipulations.

The above interchange property can be confirmed by the non-commutativity of the exchange operators. Selecting the initial state as one of the degenerate ground states,[7,67] $|\psi'_{000}(t_\mathrm{i})\rangle = \frac{1}{\sqrt{2}}(|\text{☺}\rangle|\uparrow\rangle + |\text{☹}\rangle|\downarrow\rangle)$, and let $t_{\mathrm{f}j}$ be the j-th exchange time, from Eq. (13) we have the time evolution equation to another degenerate ground state, $|\psi'_{000}(t_{\mathrm{f}j})\rangle = U(t_{\mathrm{f}j}, t_\mathrm{i}) \frac{1}{\sqrt{2}}(|\text{☺}\rangle|\uparrow\rangle + |\text{☹}\rangle|\downarrow\rangle) = \frac{1}{\sqrt{2}}[\mathrm{e}^{\mathrm{i}[\arg \psi'_{+000}(t_{\mathrm{f}j})]}|\text{☺}\rangle|\uparrow\rangle + \mathrm{e}^{\mathrm{i}[\arg \psi'_{-000}(t_{\mathrm{f}j})]}|\text{☹}\rangle|\downarrow\rangle]$ for any odd integer j. The matrix form of the time evolution equation reads

$$
\begin{aligned}
|\psi'_{000}(t_{\mathrm{f}j})\rangle &= U(t_{\mathrm{f}j}, t_\mathrm{i}) \frac{1}{\sqrt{2}} \begin{pmatrix} |\text{☺}\rangle \\ |\text{☹}\rangle \end{pmatrix} \\
&= \frac{1}{\sqrt{2}} \begin{pmatrix} \mathrm{e}^{\mathrm{i}[\arg \psi'_{+000}(t_{\mathrm{f}j})]}|\text{☺}\rangle \\ \mathrm{e}^{\mathrm{i}[\arg \psi'_{-000}(t_{\mathrm{f}j})]}|\text{☹}\rangle \end{pmatrix}, \\
U(t_{\mathrm{f}j}, t_\mathrm{i}) &= \begin{pmatrix} 0 & \mathrm{e}^{\mathrm{i}[\arg \psi'_{+000}(t_{\mathrm{f}j})]} \\ \mathrm{e}^{\mathrm{i}[\arg \psi'_{-000}(t_{\mathrm{f}j})]} & 0 \end{pmatrix}, \qquad (14)
\end{aligned}
$$

where $U(t_{\mathrm{f}j},t_{\mathrm{i}})$ is the unitary exchange operator. At time $t_{\mathrm{f}j'}$ with any even integer j', the wavepackets exchange even times and return to the initial positions, so the wave functions do not change their norms but change the phases. Thus the time evolution equation becomes

$$|\psi'_{000}(t_{\mathrm{f}j'})\rangle = U(t_{\mathrm{f}j'},t_{\mathrm{i}})\frac{1}{\sqrt{2}}\begin{pmatrix}|\circlearrowleft\rangle\\ |\circlearrowleft\rangle\end{pmatrix} = \frac{1}{\sqrt{2}}\begin{pmatrix}\mathrm{e}^{\mathrm{i}[\arg\psi'_{+000}(t_{\mathrm{f}j'})]}|\circlearrowleft\rangle\\ \mathrm{e}^{\mathrm{i}[\arg\psi'_{-000}(t_{\mathrm{f}j'})]}|\circlearrowleft\rangle\end{pmatrix},$$
$$U(t_{\mathrm{f}j'},t_{\mathrm{i}}) = \begin{pmatrix}\mathrm{e}^{\mathrm{i}[\arg\psi'_{+000}(t_{\mathrm{f}j'})]} & 0\\ 0 & \mathrm{e}^{\mathrm{i}[\arg\psi'_{-000}(t_{\mathrm{f}j'})]}\end{pmatrix}. \quad (15)$$

Clearly, non-commutativity of the exchange operators $U(t_{\mathrm{f}j},t_{\mathrm{i}})$ and $U(t_{\mathrm{f}j'},t_{\mathrm{i}})$ can be demonstrated by the calculation

$$U(t_{\mathrm{f}j},t_{\mathrm{i}})U(t_{\mathrm{f}j'},t_{\mathrm{i}}) = \begin{pmatrix}0 & \mathrm{e}^{\mathrm{i}[\arg\psi'_{+000}(t_{\mathrm{f}j})+\arg\psi'_{-000}(t_{\mathrm{f}j'})]}\\ \mathrm{e}^{\mathrm{i}[\arg\psi'_{-000}(t_{\mathrm{f}j})+\arg\psi'_{+000}(t_{\mathrm{f}j'})]} & 0\end{pmatrix}$$
$$\neq U(t_{\mathrm{f}j'},t_{\mathrm{i}})U(t_{\mathrm{f}j},t_{\mathrm{i}}) = \begin{pmatrix}0 & \mathrm{e}^{\mathrm{i}[\arg\psi'_{+000}(t_{\mathrm{f}j})+\arg\psi'_{+000}(t_{\mathrm{f}j'})]}\\ \mathrm{e}^{\mathrm{i}[\arg\psi'_{-000}(t_{\mathrm{f}j})+\arg\psi'_{-000}(t_{\mathrm{f}j'})]} & 0\end{pmatrix}, \quad (16)$$

because of the nonzero accumulated phase difference, $\arg\psi'_{+000}(t_{\mathrm{f}j'})-\arg\psi'_{-000}(t_{\mathrm{f}j'})\neq 0$. It is the different accumulated phases that make the non-Abelian-like interchange,[65,68] namely, any one of the above wavepacket-exchanged states $|\psi'_{000}(t_{\mathrm{f}j})\rangle$ and $|\psi'_{000}(t_{\mathrm{f}j'})\rangle$ behaving as quasiparticles cannot be expressed as a product of the initial state $|\psi'_{000}(t_i)\rangle$ and a phase factor. The unitary exchange operators are related to the electric field that drives the operations in Eqs. (14) and (15). That is, one can initially turn on an electric field to induce time evolutions of the system, then turn it off at time $t_{\mathrm{f}j}$ or $t_{\mathrm{f}j'}$ to complete the exchange operation.

4. Coherently controlling transitions between stationary ground states

Now we seek the stationary ground states of undriven case and focus on the transparently coherent control of transitions between them by using an ac driving to perform exchange operations of the wavepackets. Noticing the phases in stationary states $f_{n_{u(v)}}$ of Eq. (8), $\Theta_{n_{u(v)}} = -(\frac{1}{2}+n_{u(v)})t$, from Eq. (10) we know that the stationary ground state with $n_u = n_v = 0$ cannot exist for a nonzero g_0, because of the time-dependent phase factors $\mathrm{e}^{\pm\mathrm{i}g_0 t}$ in Eq. (10). However, we can see that under the modulation resonance condition[10,11] $g_0 = \frac{1}{2}(n_v-n_u)(\hbar\omega)$, the time-dependent phases of the two terms in the square brackets of Eq. (10) become the same form $-\frac{1}{2}(1+n_v+n_u)t$. Thus equation (10) becomes a set of stationary states with constant energies $E_{n_u n_v}$ and time-independent norms. The related superposition states of Eq. (2) obey the stationary Schrödinger equation $H(x)_{\varepsilon=0}|\psi_{ln_u n_v}\rangle = E_{n_u n_v}|\psi_{ln_u n_v}\rangle$. In fact, in the case $\varepsilon = 0$, the initial constant set $S_{u(v)} = [\gamma_{u(v)}(0), b_{u(v)1}(0), b_{u(v)2}(0), A_1, A_2, B_1, B_2] = [0,0,0,A,A,0,-\pi/2]$ makes the functions $f_{n_{u(v)}}$ of Eq. (8) the usual eigenstates of a harmonic oscillator. Inserting $f_{n_{u(v)}}$ into Eq. (10) and taking a minimal resonance Raman–Zeeman (or magnetic field) strength with fractional resonance $g_0 = (n_v-n_u)/2 = 1/2$ produce a set of stationary Schrödinger kitten states of Eq. (2), which contains the degenerate ground states $|\psi_{l01}(t)\rangle$ with the motional states

$$\psi_{\pm,l01} = \frac{\mathrm{e}^{\frac{\mathrm{i}}{2}(\alpha^2 t-2t\mp\phi-l\pi-2\alpha x)-\frac{1}{2}x^2}}{\pi^{\frac{1}{4}}\sqrt{2}} \times (c_u \pm c_v\sqrt{2}x\mathrm{e}^{\mathrm{i}2\alpha x+\mathrm{i}l\pi}) \quad (17)$$

for $n_u = 0$, $n_v = 1$, $l =$ even or odd number, and the normalization constants obeying $|c_u| = |c_v| = 1$. The corresponding probability densities of the particle being in spin states $|\uparrow\rangle$ and $|\downarrow\rangle$ are time-independent $|\psi_{\pm,l01}(x)|^2$. In the case of $c_u = 1$ and $c_v = \mathrm{e}^{\mathrm{i}\phi'}$, the interesting phase of Eq. (17) is analyzed in Appendix C, where the time-independent phase gradients are calculated, which contain some singular points for the special values of the parameters α and ϕ'. The phase gradient is proportional to the velocity field, and the singular points are the analogues of the 2D vortex cores[66] at which the densities vanish and phases hop for the motional states. The degenerate first excitation state reads $|\psi_{l12}\rangle$ with $n_u = 1, n_v = 2$ and different l values. Noticing $x_{u(v)} = 0$ for any eigenstate $f_{u(v)}$ of a harmonic oscillator, the eigenenergies of the stationary superposition states are given by Eq. (11) as $E_{n_u n_v} = \frac{1}{2}(1+n_u|c_u|^2+n_v|c_v|^2)-\frac{\alpha^2}{2}$. In the case of the maximal spin-motion entanglement[58] with $|c_u| = |c_v| = 1$, the lowest two levels read $E_{01} = (1-\frac{1}{2}\alpha^2)(\hbar\omega)$ and $E_{12} = (2-\frac{1}{2}\alpha^2)(\hbar\omega)$. The energy gap $\Delta E = E_{12}-E_{01} = 1(\hbar\omega)$ is relatively great compared to the perturbation level difference (e.g., see Ref. [5] for a quantum-dot-electron system). The large energy gap is important for performing the quantum logic operation. For instance, when the Raman–Zeeman (or magnetic field) strength is slightly disturbed at a moment, the produced corrected energy cannot cause transition from the ground states to the excitation states.

In many applications based on a trapped ion system without SOC, the ion can be cooled and initialized experimentally to a nearly pure and unique motional ground

state.[6,69,70] For the considered SOC system, although the degenerate ground states are not unique, we can initially prepare one of the ground states. The initial constant sets $S_{u(v)} = [\gamma_{u(v)}(0)], b_{u(v)1}(0), b_{u(v)2}(0), A_{1,2}, B_{1,2}]$ then are determined by the forms of the initial ground states.[58] It is easy to create an usual quantum transition from one of ground states $|\psi_{l01}(t)\rangle$ of different l to any excitation state with $g_0 = (n_v - n_u)/2 > 1/2$ by using a laser with resonance frequency to match the level difference ΔE. In the transition process, unclear spatiotemporal evolutions of the wavepackets are quantum-mechanically allowable. In principle, the usual quantum transition with energy exchange is equivalent to that with state transfer. However, to realize a transition among the different ground states without level difference, we have to consider how to control time evolutions of the degenerate states in a transition process with the same initial and final energy, in especial to control the time evolutions of the observable probability-density wavepackets.[7,60] Considering a simple example with $\alpha = 0.1$, $c_u = 1, c_v = e^{i\phi'} = e^{i3}$, from Eq. (17) we plot the wavepackets $|\psi_{\pm,001}(x)|^2$ and $|\psi_{\pm,101}(x)|^2$, as shown in Fig. 3. According to the definition of a kitten state, figure 3(a) with $l = 0$ is associated with an ill kitten state and figure 3(b) with $l = 1$ corresponds to its degenerate kitten state. In Fig. 3 we also show that for a fixed SOC strength the density wavepackets obey $|\psi_{+,001}|^2 = |\psi_{-,101}|^2$ and $|\psi_{-,001}|^2 = |\psi_{+,101}|^2$, and the former has zero density node $x_+ = 1/\sqrt{2}$. This means that the interchanges between the wavepackets with $l = 0$ and those with $l = 1$ imply quantum transitions between the degenerate stationary ground states.

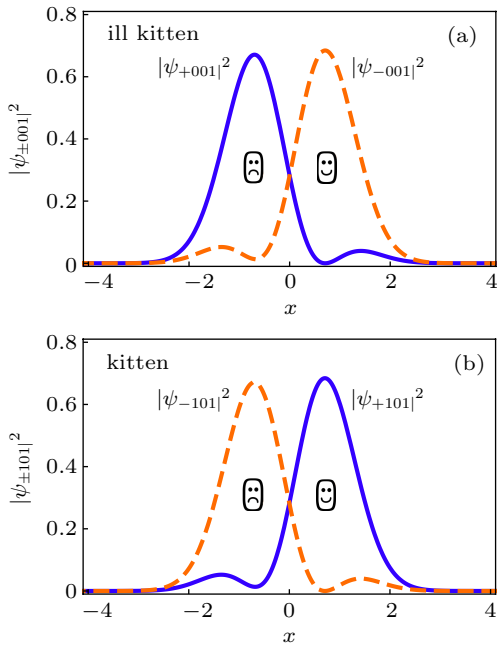


Fig. 3. Spatial distributions of the wavepackets associated with two stationary degenerate ground states for $\phi' = 3, \alpha = 0.1$: (a) wavepackets associated with an ill kitten state with $l = 0$; (b) wavepackets corresponding to a kitten state with $l = 1$. Quantum transition between these degenerate ground states can be manipulated via ac-driven interchange of the wavepackets.

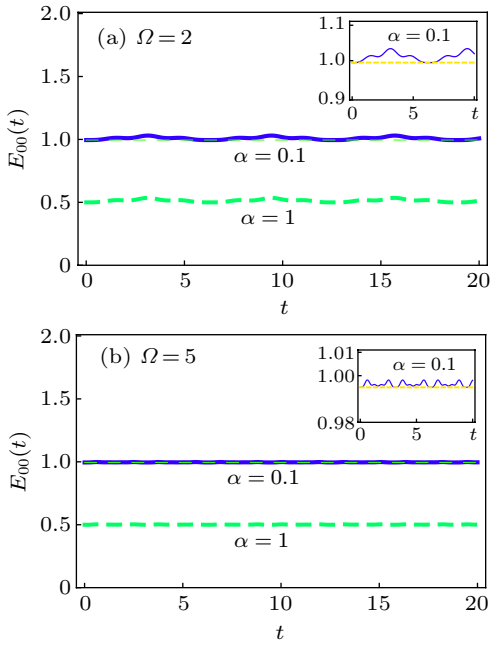


Fig. 4. (a) Time evolutions of the expected energies with the solid curve being associated with the same parameters as those of Fig. 2(a) and the dashed curve with the same parameters except for $\alpha = 1$. (b) Time evolutions of the expected energies after increasing driving frequency from $\Omega = 2$ to $\Omega = 5$. In the insets we show that the expected energy $E_{00}(t)$ for $\alpha = 0.1$ approximately equals the stationary state energy E_{01} indicated by the horizontal line, and the larger Ω value corresponds to smaller deviation from E_{01}. The dashed curves in both figures imply the similar conclusion for $\alpha = 1$.

As shown in Fig. 2(a), in an oscillating period of the wavepackets, the particle can experience many kitten and ill kitten states with different heights, widths, and distances between the corresponding wavepackets. Therefore, starting with any stationary ground state of motional states Eq. (17), after a $\pi/2$ rotation we can switch on the ac field to prepare the initial state $|\psi'_{000}(t_i)\rangle$ of Eq. (13) with norms of motional states being similar to those in Fig. 2(a), then switch off the driving at a suitable time t_f to transfer the state to $|\psi'_{000}(t_f)\rangle$ with norms of motional states being similar to those of Eq. (17) for different constants $c_{u(v)}$. For instance, starting with the stationary state with norms approximating to Fig. 3(b), we switch on the ac field at $t_i = 0$ to prepare the initial state of Fig. 2(b), then switch off the driving at $t_f = 2.6\omega^{-1}$, the system evolves to a final state of Fig. 2(b) at $t = 2.6$, which approaches to the state of Fig. 3(a). Consequently, the undriven particle will spontaneously transit to the stationary ground state with norms of Fig. 3(a). Although the accumulated phases in the driving process can be fitted by the phases of complex numbers c_u and c_v in Eq. (17), the wavepacket interchanges are only related to the wavepackets' coordinates, and the latter are determined by the norms of the motional wave functions. Particularly, such operations depend on a known final state for a given initial state, and the other states in the interchange processes can be ignored. The corresponding expectation values of energy are plotted in Fig. 4, where we show that in the process of wavepacket interchanges, for a sufficiently large driv-

ing frequency Ω the expected energy is approximately equal to and slight greater than the stationary state one with deviation being much less than the energy gap $\Delta E = 1(\hbar\omega)$. Furthermore, in the limit of a weak ac electric field and under the SOC-dependent phase-locked condition, the transition rate between the lowest two spin–orbit states with small energy gap vanishes.[5] Thus, the transitions between the degenerate ground states are robust and insensitive to the perturbations from the exchange operations. Such manipulations may be useful for controlling the degenerate ground states to perform the quantum logical operations, when the system is extend to an array of weakly coupled single-particle quantum wells.

5. Discussion and conclusion

We have investigated a single spin–orbit coupled particle subjected to an ac external field. Under the SOC-dependent phase-locked condition, we derive a set of exact spin-motion entangled Schrödinger kitten states which contains some degenerate ground states with oscillating density wavepackets. In the undriven case, the pairs of stationary wavepackets of the degenerate ground states are constructed by using a modulation resonance with the Raman–Zeeman (or magnetic field) strength fitting the trap frequency. The exchange operations with one wavepacket going through another are shown by using the ac driving, which shift the system between different ground states. The expected energy consisting of a continuous part and a quantum one is computed, and the energy deviation caused by the exchange operations is much less than the quantum gap. The ground states of Eq. (10) depend on the integer l but the energy of Eq. (11) is independent of l such that the degeneracy ground states can be created by manipulating the density wavepackets distinguished by the different l. Such degeneracy is not based on simple symmetry consideration, because of the symmetry-independent l. The symmetry-independent degeneracy ground states result in the robust spin-motion entanglement.

The exact results can be justified with the current experimental capability for a nanowire quantum-dot-electron system[3] and can be further extended to the system of trapped ions. Treating the exact solutions as the leading-order ones, the obtained results also may be directly extended to an array of particles separated from each other by different quantum wells with weak neighboring coupling as perturbation, such as the coupled magnetic atomic chain with SOC on a superconductor[72] and the spin–orbit coupled single atoms initially prepared in Mott insulating state[71] which are held in an optical lattice with a single atom at each site.[61,62] In the latter case, we can lower the lattice depth to transform the system from the tight-binding regime into the weak Lamb–Dicke regime[6,67] with harmonic trap at each well and with weak coupling between the neighbor wells. It is worth noting that the confined few-body system with controllable numbers of atoms within a given well has been realized experimentally.[61,73] The similar array of charged particles also can be the weakly coupled single-electron quantum dots with SOC. The exchange operation of wavepackets can be performed individually for any one of the single particles,[9] while the operation time for different particles can be selected to change the state of the system in a way that depends only on the order of the exchanges. These results show the decoherence-averse effect of SOC and the transparently coherent control of qubits in a 1D particle system, which could be fundamental important for encoding the spin–orbit qubits via the robust spin-motion entangled degenerate ground states.

Appendix A: Explicit forms of the motional states used in Fig. 1

When we take the parameters $|c_u| = |c_v| = 1, n_u = n_v = 0$ and the initial constant set $S_{u(v)} = [\gamma_{u(v)}(0) = b_{u(v)2}(0) = 0, b_{u1}(0) = -b_{v1}(0) = b_0, A_1 = A_2 = A, B_1 = 0, B_2 = -\pi/2]$, the auxiliary functions in Eq. (9) become

$$
\begin{aligned}
&\varphi_1(t) = A\cos t,\ \ \varphi_2(t) = A\sin t,\ \ \rho = c_0 = A,\ \ \chi = t,\ \ \xi_{u(v)} = x - b_{u(v)1}(t),\\
&b_{u1}(t) = \varepsilon\Big[\cos t\int_0^t \sin\tau\cos(\Omega\tau)\,\mathrm{d}\tau - \sin t\int_0^t \cos\tau\cos(\Omega\tau)\,\mathrm{d}\tau\Big] + b_0\cos t = b_{v1}(t) + 2b_0\cos t,\\
&b_{u2}(t) = \varepsilon\Big[-\cos t\int_0^t \cos\tau\cos(\Omega\tau)\,\mathrm{d}\tau - \sin t\int_0^t \sin\tau\cos(\Omega\tau)\,\mathrm{d}\tau\Big] - b_0\sin t = b_{v2}(t) - 2b_0\sin t,\\
&R_{0u(v)}(x,t) = \pi^{-1/4}\,\mathrm{e}^{-\xi_{u(v)}^2/2},\quad \Theta_{0u(v)}(x,t) = -\frac{1}{2}t + b_{u(v)2}x + \frac{1}{2}\int_0^t [b_{u(v)1}^2(\tau) - b_{u(v)2}^2(\tau)]\,\mathrm{d}\tau,
\end{aligned}
\tag{A1}
$$

where the integrals can be easily completed, the functions $R_{0u(v)} = R_0(S_{u(v)}, x, t)$, $\Theta_{0u(v)} = \Theta_0(S_{u(v)}, x, t)$ with different constant set $S_{u(v)}$ mean the different functions $f_{u(v)}(x,t)$ of Eq. (10). Applying these constants and functions to Eq. (10), we obtain the explicit solutions

$$
\Psi_{\pm,l00}(S_{u(v)}, x, t) = \frac{1}{\sqrt{2\sqrt{\pi}}}\,\mathrm{e}^{\frac{\mathrm{i}}{2}[\alpha^2 t \mp \phi - l\pi - 2(\alpha x + g_0 t) + 2\Theta_{0u}]}\Big[\mathrm{e}^{-\frac{1}{2}\xi_u^2} \pm \mathrm{e}^{-\frac{1}{2}\xi_v^2 + \mathrm{i}(2\alpha x + 2g_0 t + l\pi + \Theta_{0v} - \Theta_{0u} + \phi')}\Big],
$$

$$|\psi_{\pm,l00}(S_{u(v)},x,t)|^2=\frac{1}{2\sqrt{\pi}}[(\mathrm{e}^{-\xi_u^2}+\mathrm{e}^{-\xi_v^2})\pm\mathrm{e}^{-\frac{1}{2}(\xi_u^2+\xi_v^2)}\cos(2\alpha x+2g_0t+l\pi+\Theta_{0v}-\Theta_{0u}+\phi')],$$
$$\arg[\psi_{\pm,l00}(S_{u(v)},x,t)]=\arctan\left[\frac{\pm\mathrm{e}^{-\frac{1}{2}\xi_v^2}\sin(2\alpha x+2g_0t+l\pi+\Theta_{0v}-\Theta_{0u}+\phi')}{\mathrm{e}^{-\frac{1}{2}\xi_u^2}\pm\mathrm{e}^{-\frac{1}{2}\xi_v^2}\cos(2\alpha x+2g_0t+l\pi+\Theta_{0v}-\Theta_{0u}+\phi')}\right]$$
$$+\frac{1}{2}[\alpha^2t\mp\phi-l\pi-2(\alpha x+g_0t)+2\Theta_{0u}]. \tag{A2}$$

Here phase difference ϕ' between c_v and c_u and the constant set $S_{u(v)}$ are adjusted by the initial conditions determining the wavepackets. The square norms $|\psi_{\pm,l00}|^2$ of Eq. (A2) are periodic functions of time, while the phases $\arg\psi_{+,l00}$ and $\arg\psi_{-,l00}$ are obviously different and aperiodic in time for even l and odd l, respectively.

Appendix B: Explicit forms of the motional states used in Fig. 2

Combining Eq. (13) with Eq. (10) for $c_u=c_v=1$ and $\phi'=0$, we arrive at the explicit solutions after the rotation of a $\pi/2$ pulse

$$\psi'_{+,ln_un_v}(x,t)=\mathrm{e}^{\frac{\mathrm{i}}{2}(\alpha^2t-l\pi)}\left[f_{n_u}\mathrm{e}^{-\mathrm{i}(\alpha x+g_0t)}\cos\frac{\phi}{2}-\mathrm{i}f_{n_v}\mathrm{e}^{\mathrm{i}(\alpha x+g_0t+l\pi)}\sin\frac{\phi}{2}\right],$$
$$\psi'_{-,ln_un_v}(x,t)=\mathrm{e}^{\frac{\mathrm{i}}{2}(\alpha^2t-l\pi)}\left[-\mathrm{i}f_{n_u}\mathrm{e}^{-\mathrm{i}(\alpha x+g_0t)}\sin\frac{\phi}{2}+f_{n_v}\mathrm{e}^{\mathrm{i}(\alpha x+g_0t+l\pi)}\cos\frac{\phi}{2}\right]. \tag{B1}$$

The corresponding wavepackets are described by the probability densities

$$|\psi'_{+,ln_un_v}(x,t)|^2=\left[R^2_{n_u}(x,t)\cos^2\frac{\phi}{2}+R^2_{n_v}(x,t)\sin^2\frac{\phi}{2}\right]+\sin\phi\ R_{n_u}R_{n_v}\sin[\Theta_{n_u}-\Theta_{n_v}-2(\alpha x+g_0t)-l\pi],$$
$$|\psi'_{-,ln_un_v}(x,t)|^2=\left[R^2_{n_u}(x,t)\sin^2\frac{\phi}{2}+R^2_{n_v}(x,t)\cos^2\frac{\phi}{2}\right]-\sin\phi\ R_{n_u}R_{n_v}\sin[\Theta_{n_u}-\Theta_{n_v}-2(\alpha x+g_0t)-l\pi], \tag{B2}$$

which obey the normalization requirement $|\psi'_{+,ln_un_v}|^2+|\psi'_{-,ln_un_v}|^2=R^2_{n_u}+R^2_{n_v}$. Similar to Eq. (A2), the phase difference $\arg\psi'_{-,ln_un_v}-\arg\psi'_{+,ln_un_v}$ of $\psi'_{\pm,ln_un_v}(x,t)$ is also an aperiodic function of time for any set of quantum numbers, and the accumulated phase difference from the initial time t_i to the final time t_f can be nonzero that leads to non-Abelian-like interchanges of the wavepackets as quasiparticles.

Appendix C: Novel phases of the stationary motional states in Eq. (17)

Writing the phases of Eq. (17) as

$$\Phi_\pm=\arg[\psi_{\pm,l01}(x,t)]=\frac{1}{2}(\alpha^2t-2t\mp\phi-l\pi)-\alpha x+\arctan\left[\frac{\pm\sqrt{2}x\sin(2\alpha x+\phi'+l\pi)}{1\pm\sqrt{2}x\cos(2\alpha x+\phi'+l\pi)}\right], \tag{C1}$$

the accumulated phase from t_i to t_f reads $(\alpha^2-2)(t_\mathrm{f}-t_\mathrm{i})$, which is the same for $\Phi_\pm$ of the stationary states such that the accumulated phase difference vanishes for the stationary states. The time-independent phase gradients $\Phi_{\pm,x}$ contain some singular points for some values of the parameters α and ϕ'. These singular points are the analogues of the 2D vortex cores at which the densities vanish and phases hop for the motional states. The phase gradients are derived from Eq. (C1) as

$$\Phi_{\pm,x}=\frac{4\alpha x^2\pm\sqrt{2}[2\alpha x\cos(2\alpha x+\phi'+l\pi)+\sin(2\alpha x+\phi'+l\pi)]}{1+2x^2\pm2\sqrt{2}\,x\cos(2\alpha x+\phi'+l\pi)}-\alpha. \tag{C2}$$

The zero points of the denominator imply that for $\alpha=\frac{1}{\sqrt{2}}(n\pi-\phi')>0$ with $n=\pm1,\pm2,\ldots$, the singular points of $\Phi_{\pm,x}(x)$ are $x_\pm=\pm1/\sqrt{2}$, respectively. The required SOC strength is adjusted by the phase difference ϕ', and a usual zero phase difference corresponds to stronger SOC. To see the 1D novel property of the degenerate ground states, we can employ the analytic prolongation (see, e.g. Ref. [73]) on the complex plane, $\Phi_{\pm,x}(z)$ for $z=x+\mathrm{i}y$, to construct the circulation integrals $\oint_{\Gamma_\pm}\Phi_{\pm,x}(z)\mathrm{d}z=2\pi\mathrm{i}\times\mathrm{res}\Phi_{\pm,x}(z_\pm)=2N\pi$ for the topological charges $N=0,\pm1,\pm2,\ldots$. Here $\Gamma_\pm$ are closed trajectories enclosing the poles $z_\pm=x_\pm$ and the res denotes the residues at the poles. Various topologically equivalent closed trajectories are allowable for any one of the above circulation integral.

References

[1] Nowack K C, Koppens F H L, Nazarov Y V and Vandersypen L M K 2007 *Science* **318** 1430
[2] Nadj-Perge S, Frolov S M, Bakkers E P A M and Kouwenhoven L P 2010 *Nature* **468** 1084
[3] Mourik V, Zuo K, Frolov S M, Plissard S R, Bakkers E P A M and Kouwenhoven L P 2012 *Science* **336** 1003
[4] Pioro-Ladrière M, Obata T, Tokura Y, Shin Y S, Kubo T, Yoshida K, Taniyama T and Tarucha S 2008 *Nat. Phys.* **4** 776
[5] Li R, You J Q, Sun C P and Nori F 2013 *Phys. Rev. Lett.* **111** 086805
[6] Leibfried D, Blatt R, Monroe C and Wineland D 2003 *Rev. Mod. Phys.* **75** 281
[7] Monroe C, Meekhof D M, King B E and Wineland D 1996 *Science* **272** 1131
[8] Kitagawa K, Takayama T, Matsumoto Y, Kato A, Takano R, Kishimoto Y, Bette S, Dinnebier R, Jackeli G and Takagi H 2018 *Nature* **554** 341
[9] Loss D and DiVincenzo D P 1998 *Phys. Rev. A* **57** 120
[10] Kato Y, Myers R C, Driscoll D C, Gossard A C, Levy J and Awschalom D D 2003 *Science* **299** 1201
[11] Rashba E I and Efros A L 2003 *Phys. Rev. Lett.* **91** 126405
[12] Wang K, Li H O, Xiao M, Cao G and Guo G P 2018 *Chin. Phys. B* **27** 090308
[13] Lin Y J, Jimenez-Garcia K and Spielman I B 2011 *Nature* **471** 83
[14] Wu Z, Zhang L, Sun W, Xu X T, Wang B Z, Ji SC, Deng Y j, Chen S, Liu X J and Pan J W 2016 *Science* **354** 83
[15] Zhang Y P, Mao L and Zhang C W 2012 *Phys. Rev. Lett.* **108** 035302
[16] Hu F Q, Wang J J, Yu Z F, Zhang A X and Xue J K 2016 *Phys. Rev. E* **93** 022214
[17] Salasnich L and Malomed B A 2013 *Phys. Rev. A* **87** 063625
[18] Zhu C Z, Dong L and Pu H 2016 *J. Phys. B* **49** 145301
[19] Cheng Y S, Tang G H and Adhikari S K 2014 *Phys. Rev. A* **89** 063602
[20] Sun F X, Zhang W, He Q Y and Gong Q H 2018 *Phys. Rev. A* **97** 012307
[21] Zhang D W, Fu L B, Wang Z D and Zhu S. L 2012 *Phys. Rev. A* **85** 043609
[22] Garcia-March M A, Mazzarella G, Dell'Anna L, Juliá-Díaz B, Salasnich L and Polls A 2014 *Phys. Rev. A* **89** 063607
[23] Sun F, Ye J and Liu W M 2017 *New J. Phys.* **19** 063025
[24] Yang S, Wu F, Yi W and Zhang P 2019 *Phys. Rev. A* **100** 043601
[25] Xie W F, He Y Z and Bao C G 2015 *Chin. Phys. B* **24** 060305
[26] Kong C, Chen H, Li C and Hai W 2018 *Chaos* **28** 023115
[27] Kong C, Luo X, Chen H, Luo Y and Hai W 2019 *Chaos* **29** 103148
[28] Lü H, Zhu S B, Qian J and Wang Y Z 2015 *Chin. Phys. B* **24** 090308
[29] Liu W M and Li J 2018 *Acta Phys. Sin.* **67** 110302 (in Chinese)
[30] Zhang H F, Chen F, Yu C C, Sun L H and Xu D H 2017 *Chin. Phys. B* **26** 080304
[31] Li H and Chen F L 2019 *Chin. Phys. B* **28** 070302
[32] Xu Z F and You L 2012 *Phys. Rev. A* **85** 043605
[33] Tsitsishvili E, Lozano G S and Gogolin A O 2004 *Phys. Rev. B* **70** 115316
[34] Salerno M, Abdullaev F Kh, Gammal A and Tomio L 2016 *Phys. Rev. A* **94** 043602
[35] Jiménez-García K, LeBlanc L J, Williams R A, Beeler M C, Qu C, Gong M, Zhang C and Spielman I B 2015 *Phys. Rev. Lett.* **114** 125301
[36] Grusdt F, Li T, Bloch I and Demler E 2017 *Phys. Rev. A* **95** 063617
[37] Kartashov Y V, Konotop V V and Vysloukh V A 2018 *Phys. Rev. A* **97** 063609
[38] Soluyanov A A, Gresch D, Troyer M, Lutchyn R M, Bauer B and Nayak C 2016 *Phys. Rev. B* **93** 115317
[39] Combescot M, Shiau S Y and Voliotis V 2019 *Phys. Rev. B* **99** 245202
[40] Liu X J, Borunda M F, Liu X and Sinova J 2009 *Phys. Rev. Lett.* **102** 046402
[41] Guan Q and Blume D 2015 *Phys. Rev. A* **92** 023641
[42] Li C, Ye F, Chen X, Kartashov Y V, Torner L and Konotop V V 2018 *Phys. Rev. A* **98** 061601
[43] Zener C 1932 *Proc. R. Soc. A* **137** 696
[44] Rabi I 1937 *Phys. Rev.* **51** 652
[45] McCall S L and Hahn E L 1969 *Phys. Rev.* **183** 457
[46] Bambini A and Berman P R 1981 *Phys. Rev. A* **23** 2496
[47] Kyoseva E S and Vitanov N V 2005 *Phys. Rev. A* **71** 054102
[48] Xie Q and Hai W 2010 *Phys. Rev. A* **82** 032117
[49] Barnes E and Das Sarma S 2012 *Phys. Rev. Lett.* **109** 060401
[50] Hai W, Hai K and Chen Q 2013 *Phys. Rev. A* **87** 023403
[51] Luo X, Yang B, Zhang X, Li L and Yu X 2017 *Phys. Rev. A* **95** 052128
[52] Li Z, Hai W and Deng Y 2013 *Chin. Phys. B* **22** 090505
[53] Fielding H, Shapiro M and Baumert T 2008 *J. Phys. B* **41** 070201
[54] Wei Y, Kong C and Hai W 2019 *Chin. Phys. B* **28** 056701
[55] Nowak M P and Szafran B 2013 *Phys. Rev. B* **87** 205436
[56] Hai W, Xie Q and Fang J 2005 *Phys. Rev. A* **72** 012116
[57] Lu G, Hai W and Xie Q 2006 *J. Phys. A* **39** 401
[58] Hai K, Luo Y, Chong G, Chen H and Hai W 2017 *Quantum Inf. Comput.* **17** 456
[59] Ourjoumtsev A, Tualle-Brouri R, Laurat J and Grangier P 2006 *Sciences* **312** 83
[60] Kienzler D, Fluhmann C, Negnevitsky V, Lo H Y, Marinelli M, Nadlinger D and Home J P 2016 *Phys. Rev. Lett.* **116** 140402
[61] Cheinet P, Trotzky S, Feld M, Schnorrberger U, Moreno-Cardoner M, Fölling S and Bloch I 2008 *Phys. Rev. Lett.* **101** 090404
[62] Luo Y, Lu G, Kong C and Hai W 2016 *Phys. Rev. A* **93** 043409
[63] Ma R, Tai M E, Preiss P M, Bakr W S, Simon J and Greiner M 2011 *Phys. Rev. Lett.* **107** 095301
[64] Chen Y A, Nascimbene S, Aidelsburger M, Atala M, Trotzky S and Bloch I 2011 *Phys. Rev. Lett.* **107** 210405
[65] Stern A 2010 *Nature* **464** 187
[66] Hai W, Lee C and Zhu Q 2008 *J. Phys. B* **41** 095301
[67] Gardiner S A, Cirac J I and Zoller P 1997 *Phys. Rev. Lett.* **79** 4790
[68] Chen H, Kong C, Hai K and Hai W 2019 *Quantum Inf. Proc.* **18** 379
[69] Mizrahi J, Senko C, Neyenhuis B, Johnson K G, Campbell W C, Conover C W S and Monroe C 2013 *Phys. Rev. Lett.* **110** 203001
[70] Hayes D, Matsukevich D N, Maunz P, Hucul D, Quraishi Q, Olmschenk S, Campbell W, Mizrahi J, Senko C and Monroe C 2010 *Phys. Rev. Lett.* **104** 140501
[71] Cole W S, Zhang S, Paramekanti A and Trivedi N 2012 *Phys. Rev. Lett.* **109** 085302
[72] Xiao J P and An J 2015 *New J. Phys.* **17** 113034
[73] Esmann M, Teichmann N and Weiss C 2011 *Phys. Rev. A* **83** 063634
[74] Goldstein H 1980 *Classical Mechanics* (New York: Addison-Weslay Publishing Co.) Chap. **10**